



Vacuum membrane distillation–crystallization process of high ammonium salt solutions

Wen-Ting You, Zhen-Liang Xu*, Zhe-Qin Dong, Mi Zhang

State Key Laboratory of Chemical Engineering, Membrane Science and Engineering R&D Lab, Chemical Engineering Research Center, East China University of Science and Technology (ECUST), 130 Meilong Road, Shanghai 200237, China, Tel. +86 21 64253061; Fax: +86 21 64252989; emails: yoyo3144@163.com (W.-T. You), chemxuzl@ecust.edu.cn (Z.-L. Xu), pizid@126.com (Z.-Q. Dong), mizhang0226@163.com (M. Zhang)

Received 12 November 2013; Accepted 13 April 2014

ABSTRACT

The batch mode of vacuum membrane distillation–crystallization (VMDC) process was carried out in the ammonium salt solutions. Vacuum membrane distillation (VMD) was used to permeate water to a desired concentration and the crystallizer was applied for the precipitation of crystals. The influence of concentration time on the permeate flux was investigated and the transfer resistances were estimated. Membrane fouling resistance increased gradually when the solution was concentrated up to the critical point of supersaturation factor. Beyond this critical point, the NH_4Cl system revealed an irreversible membrane fouling, whereas the $(\text{NH}_4)_2\text{SO}_4$ system revealed a reversible membrane fouling. By analyzing the transfer resistances, the determining concentration in the VMD process could be obtained, which would provide a way of avoiding membrane fouling problem. The permeated total nitrogen (TN) increased significantly from 4.7 to 59.8 mg/L with the NH_4Cl solution. However, low level permeated TN ($\text{TN} < 3 \text{ mg/L}$) with $(\text{NH}_4)_2\text{SO}_4$ solution was maintained during the whole concentration process. The NH_4Cl crystals with dendritic structure and $(\text{NH}_4)_2\text{SO}_4$ crystals of lamellar form were obtained by the crystallizer with the production of 125.7 and 58.4 kg/m³, respectively.

Keywords: Membrane distillation–crystallization; Ammonium salt; Transfer resistances

1. Introduction

Large volumes of wastewater, such as rare-earth wastewater and fertilizer plant wastewater generated from industrial activities and intensive agriculture, usually contain large amounts of ammonium salt. The massively discharged wastewater with high $\text{NH}_4\text{-N}$ concentration was in need of attention [1]. Natural water contamination by ammonium salt would lead to series of environmental problems, such as

eutrophication and ecology destroying [2,3]. However, ammonium salt was widely used in agricultural fertilizer and industry. For economic and environmental reasons, simultaneously separating pure water from wastewater and recovering ammonium salts is advantageous.

Membrane distillation crystallization (MDC) could be used in treating solutions with large amount of ammonium salt due to its potentials of valuable salts recovering and high salt wastewater desalinating. MDC was a coupling process including membrane

*Corresponding author.

distillation (MD) and crystallizer. Pure water was generated as permeate from MD process and the concentrated solutes could be recovered as crystals from the crystallizer [4–6]. In recent years, MDC process has been investigated in many studies for brine concentration and salt recovery. Gryta [7] utilized the MDC process to concentrate NaCl solution in both batch and continuous mode. The maximum NaCl concentration amounting to 320 g/L was obtained in the batch mode. Moreover, 100 kg/m³/d of NaCl crystals were separated in the crystallizer through the continuous concentration process. Tun et al. [8] employed the MDC process to produce anhydrous Na₂SO₄ with average size of 60–80 μm in batch mode, and the results showed that MD could be operated at slightly higher degrees of saturation due to the negative solubility-temperature coefficient of Na₂SO₄. Ji et al. [9] illustrated that MDC was used to produce 21 kg/m³ of NaCl with size of 20–200 μm and to recover 90% of water with artificial RO brine.

As mentioned above, the application of MDC was mainly focused on the variety of flux with the operation time and on the size and yield of recovered crystal. However, the membrane fouling resistance, which might occur in the concentration process for crystallizing solutes by MD process, should be taken into consideration. At present, the transfer resistances in MD process were investigated as follows. Srisurichan et al. [10] reported that the cake filtration model could be used to describe the fouling by the humic acid precipitation. A systematic evaluation of individual mass transfer resistances was analyzed with air gap membrane distillation and direct contact membrane distillation processes by Alkhalbi and Lior [11]. The effects of the varied operating conditions on the mass transfer resistances were investigated. Ding et al. [12] pointed out that fouling of membrane could be efficiently limited by increasing the feed temperature and flow rate. These researches provided the calculation method for resistances estimation. However, very little attention has been paid to the relationship between the transfer resistances and the solution supersaturation factor (SF) in the concentration process by MD.

In this paper, the batch mode of vacuum membrane distillation–crystallization (VMDC) process was used to treat the ammonium salt solutions of NH₄Cl and (NH₄)₂SO₄ under acidic conditions. This study focused on the relationship between the SF and individual transfer resistances. The empirical equations were applied to calculate the predicted flux and to estimate the transfer resistances. Moreover, the concentration of permeated total nitrogen (TN) which indicated the quality of permeate was also investigated.

2. Theory

2.1. Mass and heat transfer in VMD

The permeate flux J is linearly related to the difference of partial pressure across the membrane, defined as [13]:

$$J = K_m(P_m - P_v) \quad (1)$$

where P_m is the partial vapor pressure at the temperature of membrane surface, as shown in Eq. (2) and P_v is the vacuum pressure.

$$P_m = P_{sat}(T_m)\gamma(T_m)x_m \quad (2)$$

where $P_{sat}(T_m)$ calculated by the Antoine's equation is the vapor pressure of water at membrane surface temperature T_m , $\gamma(T_m)$ is the activity coefficient of water and x_m is the molar fraction of water at membrane surface.

Moreover, K_m is the MD coefficient in Eq. (1), which depends on temperature and the membrane geometric characteristics. According to the kinetic theory of dusty-gas model, two mechanisms of Knudsen diffusion and molecular diffusion are taken place in the process of the vapor transporting through the membrane pores. As reported in the previous studies [14–16], the Knudsen diffusion of water molecules is dominant in VMD process, and K_m can be written:

$$K_m = \frac{8 \varepsilon r}{3 \tau \delta} \sqrt{\frac{1}{2\pi RT_m M}} \quad (3)$$

where ε is the porosity of the membrane, r is the size of membrane pore, τ is the pore tortuosity, δ is the membrane thickness, R is the gas constant, T_m is the temperature on membrane surface, and M is the water molecular mass.

The temperature on membrane surface (T_m) and the molar fraction of water on the feed surface of membrane (x_m) are different from the corresponding bulk ones, due to the polarization effects of both temperature and concentrations in the feed boundary layer [16]. A large amount of heat is supplied to vaporize the liquid, therefore, T_m can be calculated by the amount of heat for permeate flux as shown in Eq. (4).

$$J_w \Delta H = h_f(T_b - T_m) \quad (4)$$

where h_f is the heat transfer coefficient of the VMD feed boundary layer, ΔH is the latent heat of vaporization of water, and T_b is the bulk temperature. In fact, the heat transfer coefficient can be obtained by Eq. (5).

$$h_f = \frac{Nu\mu}{d_h} \quad (5)$$

where Nu can be described by empirical Eq. (6), it was obtained by means of linear regression in Mengual [17].

$$Nu = 0.0142Re^{0.74}Pr^{0.33} \quad (6)$$

where Re and Pr are the Reynolds and Prandtl numbers, respectively.

The concentration polarization coefficient (CPC) is obtained for estimating the concentration at the membrane surface by Eq. (7),

$$\frac{C_m}{C_f} = \exp\left(\frac{J}{\rho k}\right) \quad (7)$$

where C_f is the salt concentration in the bulk, and ρ is the density of solution. The mass transfer coefficient of k is estimated in laminar regime by the Leveque equation:

$$k = 1.62 D_{self}^{2/3} \left(\frac{v}{d_h l}\right)^{1/3} \quad (8)$$

where D_{self} is the diffusion coefficient and v is the solution velocity.

According to Eqs. (1–8), the predicted flux can be obtained by the iteration method, which should assume the temperature and the value of CPC on membrane surface (T_m) first.

2.2. Transfer resistances

In the concentration process by VMD, analogous to the other forms of MD, the total resistance is the addition of three items, which are the resistance in feed boundary layer (R_b), the resistance in the fouling layer (R_f), and the resistance of membrane (R_m), respectively. The transmembrane vapor pressure difference is the driving force for the liquid through the membrane in MD process [10]. This means that the transfer resistance can be defined as the ratio between the vapor pressure difference and the permeate flux (J) as follows:

Feed boundary layer resistance:

$$R_b = \frac{P_b - P_f}{J} \quad (9)$$

Fouling layer resistance:

$$R_f = \frac{P_f - P_m}{J} \quad (10)$$

Membrane resistance:

$$R_m = \frac{P_m - P_v}{J} \quad (11)$$

Total resistance:

$$R_t = R_b + R_f + R_m = \frac{P_b - P_v}{J} \quad (12)$$

Combined with Eq. (1), R_m is the reciprocal of K_m , which is the function of T_m and the structural parameter of membrane. Therefore, the value of membrane resistance obtained from the pure water experiment was considered to be constant at the same operation condition. The variables $P_b(T_b)$, $P_f(T_f)$, and $P_m(T_m)$ related to the temperature are the vapor pressures in the bulk feed, on the fouling layer and at the boundary layer, respectively. Therefore, T_m can be evaluated from Eq. (11) and T_f can be obtained by the iteration method.

3. Experimental section

3.1. The membrane module and the batch mode of VMDC

Hydrophobic polytetrafluoroethylene (PTFE) flat-sheet membrane (membrane area was 0.0078 m², mean pore size was 0.1 μm, membrane thickness was 81 μm, and porosity is 70%) manufactured by Sumitomo Electric Industries, Ltd. was used in the experiments and the VMDC experiments were carried out in a lab scale.

The VMDC experimental installation of this work is given in Fig. 1. In VMD process, the feed water was driven by a circulation pump (Nanjing Lvhuang Pumps Co., Ltd.) and the feed flow was measured by a flow meter with precision ±2% connected between the pump and the module. A thermostatic bath was used to provide the feed with heat energy to perform VMD. The temperature of the feed water at the inlet of the membrane module was continuously measured by a Pt100 probe, which was connected to an automatic temperature regulator.

At the permeate side of the membrane module, a vacuum pump (Shanghai Vacdo Vacuum Equipment Co., Ltd.) with a pressure controller was connected to

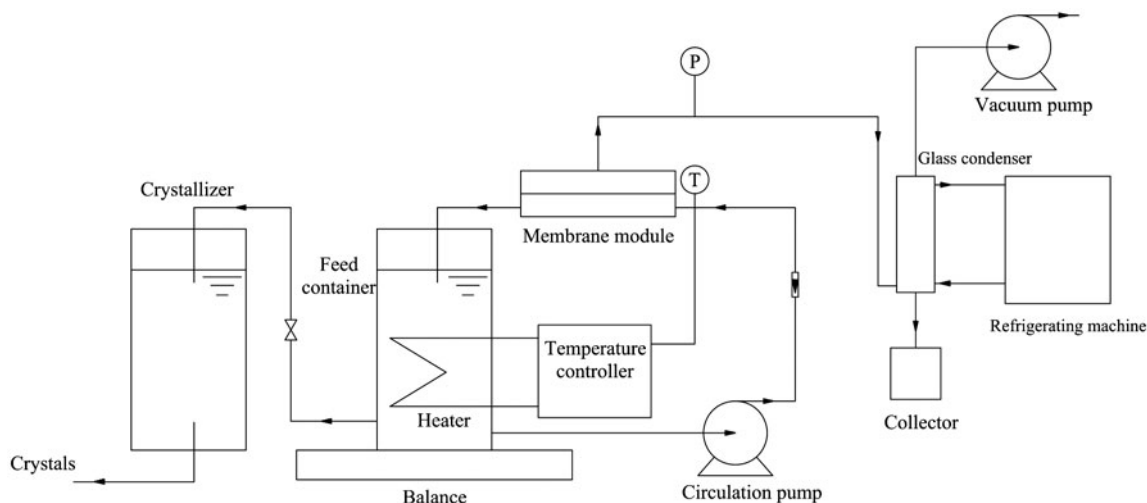


Fig. 1. Equipment of VMDC process.

remove the permeate flux. The glass condenser coupled with the refrigerating machine was used in series for water permeating vapor recovery. The permeate pressure was measured by the mercurial pressure gage. The permeate flux was calculated by measuring the volume of the condensed water in every case.

The crystallizer was used to produce crystals after the concentration of the solutions by VMD. The feed solutions with different concentrations were left to stand for 8 h cooling at room temperature (283 K) for deposition of solute crystals. The seed crystal was used in the $(\text{NH}_4)_2\text{SO}_4$ system when the solution temperature was stable. The precipitated crystals were filtered and weighted.

3.2. The ammonium salt solution

The NH_4Cl solution and the $(\text{NH}_4)_2\text{SO}_4$ solution with the initial concentrations of 20 and 34% were used as feed solutions. The pH value of the feed was adjusted at 3. The DDS-11A conductance meter (Shanghai Neici Instrument Company) was used to measure the salt concentration.

3.3. The concentration process by VMD

The feed solutions with 2.3 L were concentrated by VMD process. The feed flow rate and the pressure at the permeate side varied in the range of 21–90 L/h and 5–13 kPa, respectively. The volume of permeate was measured at each 30–50 min interval until the flux was lower than 4 L/h/m^2 .

3.4. Analytic methods

The permeate flux (J , L/h/m^2) was calculated by Eq. (13).

$$J = \frac{V}{A \times t} \quad (13)$$

where V is the permeate volume (L), A is the membrane area (m^2), and t is the microfiltration time (h).

The feed concentrations of salt was measured by DDS-11A conductance meter (Shanghai Neici Instrument Company) and calculated from the calibration curves, which were obtained on the basis of measurements with the reference solutions. Due to the high concentration of salt, the examined samples were diluted with pure water before analysis.

The TN was considered to be ammonia nitrogen due to the lack of nitrate nitrogen in this study. The permeate concentration of TN was measured by TNM-1 (SHIMADZU).

Images of the new membrane and the fouled membrane were obtained by SEM.

The crystals were visually analyzed through optical microscopy with camera connected to computer (OLYMPUS BX51).

4. Results and discussion

4.1. Concentration process by VMD

4.1.1. The changes of permeate flux

Permeate flux as a function of operating time is illustrated in Figs. 2 and 3 for the concentration

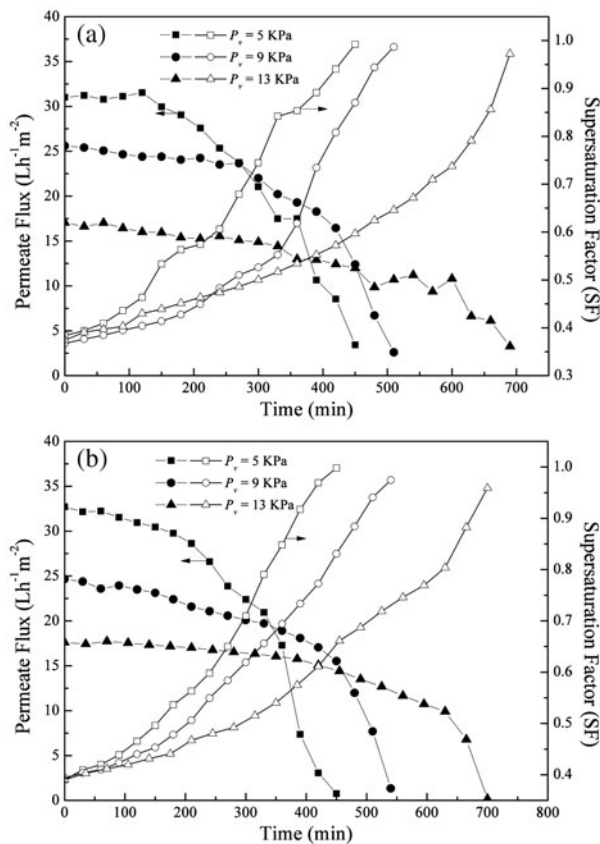


Fig. 2. Ammonium salt solution concentration process at different permeate pressures (P_v): (a) NH_4Cl system; (b) $(\text{NH}_4)_2\text{SO}_4$ system.

process of NH_4Cl solution and $(\text{NH}_4)_2\text{SO}_4$ solution. SF of feed solution was also shown. SF was the ratio between the concentration of the feed solution and the saturation concentration at the feed temperature. It is clearly observed in Figs. 2 and 3 that the decline of permeate flux can be divided into two parts along with the operating time. In the first part, a slight decline of permeate flux was observed, which was related to the increase of feed concentration with time. Higher feed solution concentration would cause higher salt mole fractions and lower activity coefficients of solvent, which would lead to lower vapor partial pressure. However, the feed concentration increased slowly during the initial period of the experiment, which lead to the slight decrease of permeate flux. A rapid permeate flux decline was observed in the second part. The increase rate of the feed concentration increased with the growth of concentration factor. In addition, when the feed solution was close to saturation (SF closes to 1), the membrane fouling occurred since the crystal was salted out and

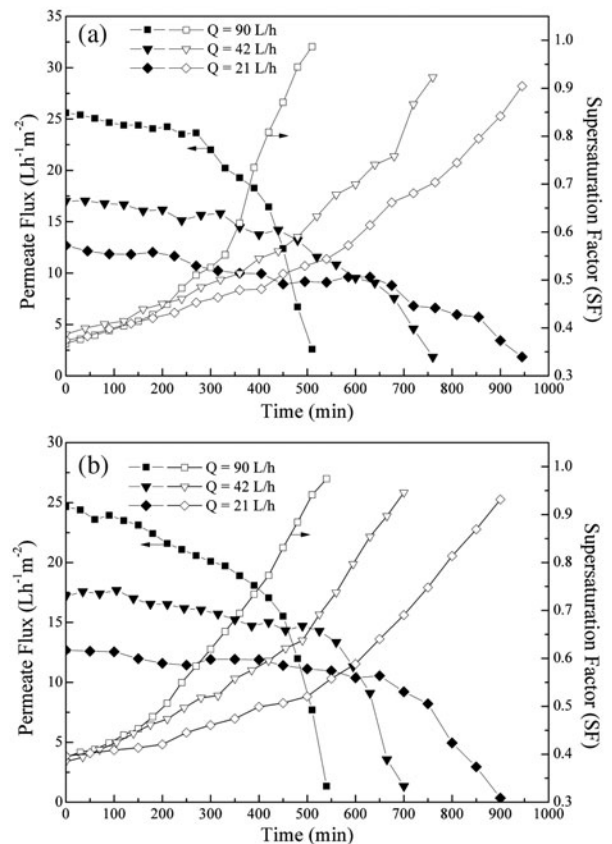


Fig. 3. Ammonium salt solution concentration process at different flow rates (Q): (a) NH_4Cl system; (b) $(\text{NH}_4)_2\text{SO}_4$ system.

precipitated at the membrane surface. Therefore, the permeate flux dropped rapidly at the end of the experiment.

Fig. 2 indicates that higher water flux through the membrane is achieved in both systems at lower permeate pressure. In the NH_4Cl system, the initial permeate flux increases from 17 to $31 \text{ L}/\text{h}/\text{m}^2$ with the decrease of the permeate pressure from 13 to 5 kPa. The permeate pressure decreased due to the increase of vapor pressure difference across both sides of the membrane pore, which strengthened the driving force. Fig. 3 shows that the initial permeate flux increased from 12.7 to $25.6 \text{ L}/\text{h}/\text{m}^2$ in the NH_4Cl system when the flow increases from 21 L/h to 90 L/h. The similar trends in flux with feed flow were observed in $(\text{NH}_4)_2\text{SO}_4$ system. In the VMD process, the large amount of heat requirement for vaporizing water at the membrane surface causes the difference of temperature between the feed solution and the membrane surface, which resulted in the temperature polarization. However, high temperature enhances

partial pressure at the membrane surface, which would lead to the increasing permeate flux. Thus, larger amount of heat would be needed to enhance the permeate flux at membrane surface. Moreover, the concentration polarization also occurred on the boundary layer. The salt concentration at membrane surface was higher than that in the feed solution. The mass and heat transfer coefficients increased since higher flow rate promoted more turbulence and eddies in the boundary layer, which lower the temperature and concentration differences between feed solution and membrane surface. Therefore, high flow rate would increase permeate flux and shortens the concentration time.

4.1.2. The changes of permeate TN concentration

It has been proved previously that the hydrolysis of ammonium ion could produce volatile ammonia in aqueous solutions [18,19]. In the process of VMD, only gas was allowed to transport through the membrane pores due to the hydrophobic property of membrane material. Large quantity of NH_3 molecules could be obtained in the permeate side with high feed pH value and high feed temperature [20–22].

However, in this experiment, the ammonium salts were rejected and concentrated to its saturation in order to produce the pure water and recover the ammonium salt crystal. According to the previous researches [18], lower feed pH value would result in a reduction of volatile ammonia. In this study, the feed pH value was controlled at about 3. However, the permeate concentration of TN still needs to be investigated due to the possibility of the producing volatile ammonia. As shown in Fig. 4, the TN concentration of permeate maintained below 3 mg/L in the $(\text{NH}_4)_2\text{SO}_4$ system. However, in the NH_4Cl system, the TN concentration of permeate maintained in the range of 3.2–4.7 mg/L at the initial 360 min, while the TN concentration of permeate increased sharply and reached to 59.8 mg/L at the end of experiment. Moreover, the variations of feed pH value with concentration time were different between two ammonium salt systems, as shown in Fig. 5. The feed pH values increased with the concentration time in the NH_4Cl system and were adjusted by acid. However, the feed pH values decline in the $(\text{NH}_4)_2\text{SO}_4$ system. This behavior was attributed to the volatile HCl produced by large quantity of H^+ and Cl^- at the liquid–vapor interface, which spreads through the membrane pores when the feed pH value was 3. Therefore, the volatile NH_3 was promoted by the production of volatile HCl under acidic conditions. Furthermore, the volatilities of NH_3 and HCl were greater than that of water. It resulted in the slower decline rate of both the NH_3 and HCl partial pressures

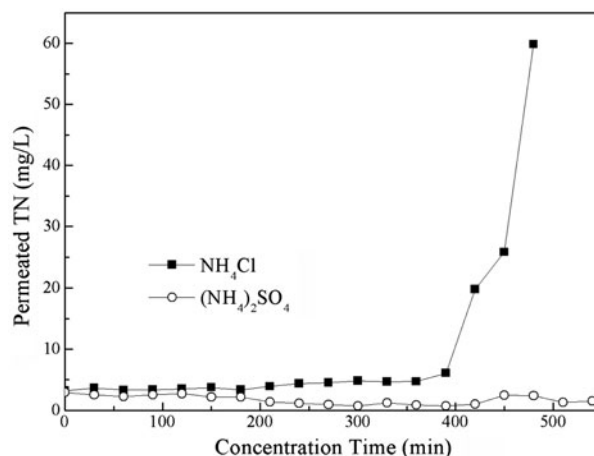


Fig. 4. TN concentration in the permeate vs. concentration time (operating condition: $P_v = 9$ kPa, $Q = 90$ L/h, $T_f = 333$ K).

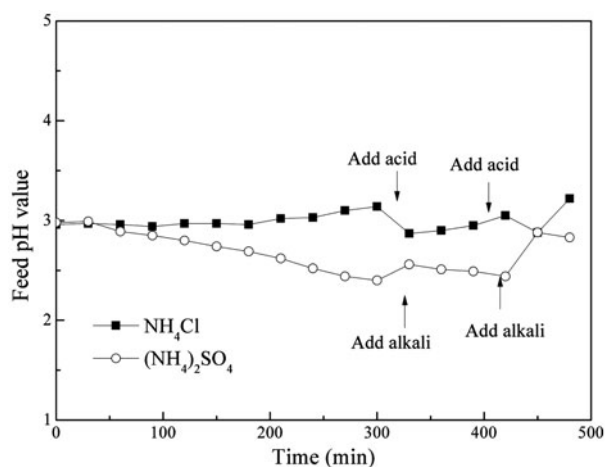


Fig. 5. The pH value in the feed vs. concentration time (operating condition: $P_v = 9$ kPa, $Q = 90$ L/h, $T_f = 333$ K).

than that of water at membrane pore entries when the solution concentration closed to the saturation concentration. It could be concluded that the anionic property in the acidic condition was an important factor that would affect the NH_3 transfer in the ammonium salt concentration process by VMD.

4.2. Transport resistances analysis of VMD in concentration process

4.2.1. Pure water system

Fig. 6(a) shows the permeate flux as function of the feed temperature and feed flow rate. Each line represents the predicted flux, and the points represent the experimental data at the same operation conditions. A

good agreement between the predicted values and the experimental data was observed. It was obvious that higher feed temperature and higher flow rate lead to higher permeate flux. As mentioned previously, the increased flow rate would decrease the effect of temperature polarization and increases the mass and heat

transfer. Therefore, higher flow rate could result in a higher flux.

As shown in Fig. 6(b), the influences of flow rate and the feed temperature on the membrane resistance (R_m) were small. The value of R_m is in the range of 162–164.7. R_m increases slightly with the increasing feed temperature. The reason behind that Knudsen diffusion was dominant in VMD process. According to the research by Martínez-Díez and Florido-Díaz [23], the influence of feed temperature on R_m with Knudsen diffusion was much less than that with molecular diffusion. However, lower flow rate would lead to higher feed boundary layer resistance (R_b). The results are shown in Fig. 6(c). Compared with higher flow rate ($Q=90$ L/h), the influence of lower flow rate ($Q=18$ L/h) on R_b is more significant. R_b increases about three times, when the flow rate increases from 18 to 90 L/h. Furthermore, Fig. 6(c) also indicates that R_b increases with the increasing of feed temperature. It suggested that greater permeate flux would contribute to larger temperature difference between bulk and membrane surface, and result in the greater influence of temperature polarization.

4.2.2. Ammonium salt solution systems

The calculated transfer resistances under the operating conditions ($P_v=9$ kPa, $Q=90$ L/h) are given in Fig. 7. Moreover, the SF at membrane surface (SF_m) was also estimated by Eq. (14) as shown in Fig. 7. The result indicated that SF_m was higher than SF at the same operation conditions, since the phenomenon of the temperature and concentration polarizations would lead to the higher concentration and the lower temperature at membrane surface than that at feed solution. Furthermore, Fig. 7 also shows that both R_m and R_b were the main transfer resistances as the feed SF_m increased up to some level, which was considered as the critical point. The estimated values of SF_m at the critical point were 0.99 and 0.98 in the NH_4Cl and the $(\text{NH}_4)_2\text{SO}_4$ system, respectively. The corresponding values of SF in the NH_4Cl and the $(\text{NH}_4)_2\text{SO}_4$ systems were 0.87 and 0.88, respectively. However, the membrane fouling resistance (R_f) grew rapidly and dominated the total resistance, which means that some membrane fouling possibly occurred when the feed SF_m was formed beyond the critical point.

$$\text{SF}_m = \frac{C_m}{C_{eq}(T_m)} \quad (14)$$

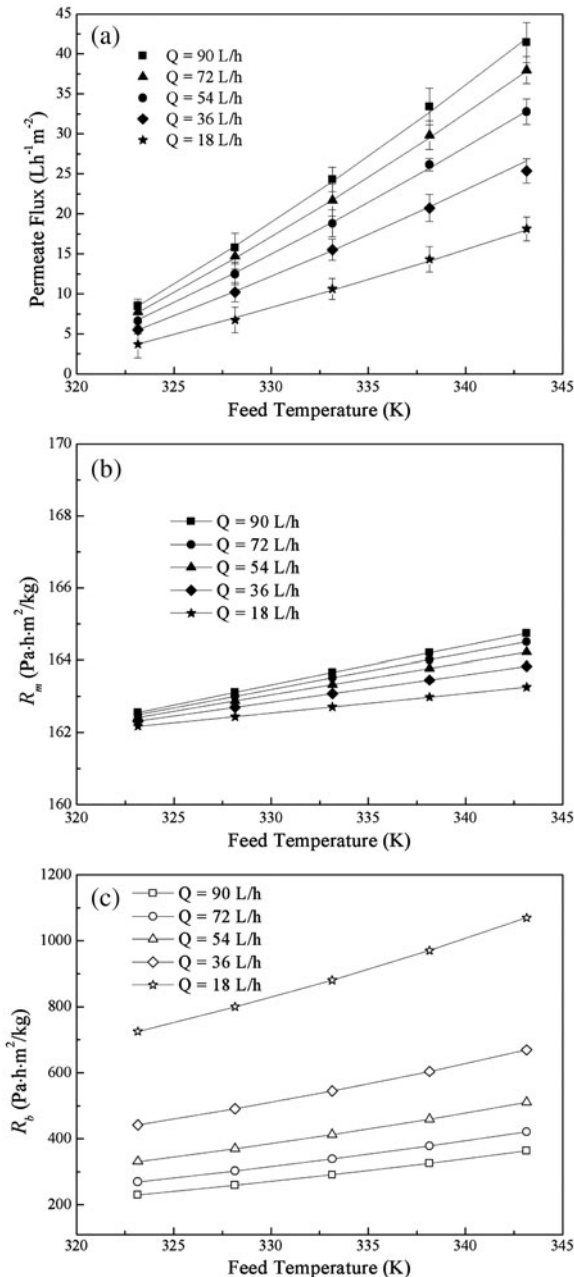


Fig. 6. VMD process with pure water as function of the feed temperature and feed flow rate ($P_v=9$ kPa): (a) the experimental data of permeate flux vs. the predicted flux; (b) the estimated membrane resistance (R_m); (c) the estimated boundary layer resistance (R_b).

Fig. 8 shows that the permeate flux vs. operating time as a function of feed SF with NH_4Cl and $(\text{NH}_4)_2\text{SO}_4$. The result indicated that the permeate flux decreased

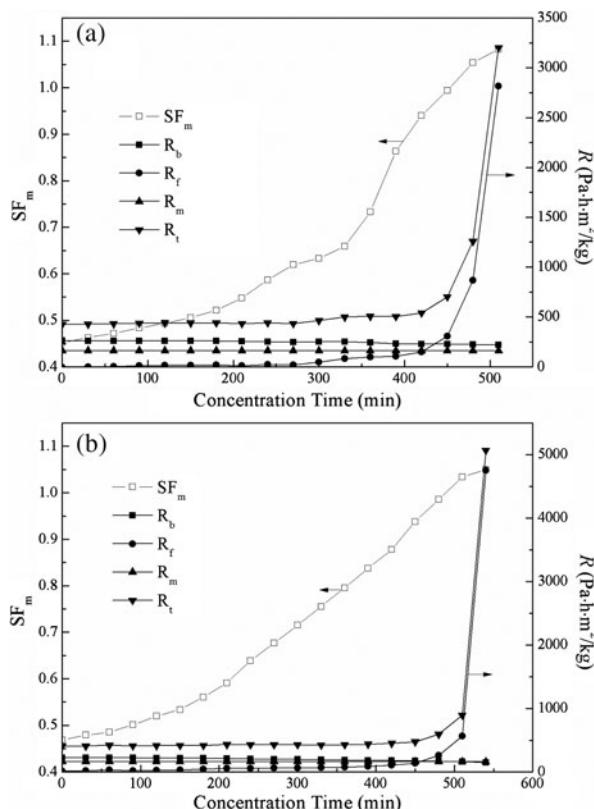


Fig. 7. The estimated transfer resistances and the SF at membrane surface (SF_m) vs. concentration time (operating condition: $P_v=9$ kPa, $Q=90$ L/h, $T_f=333$ K): (a) NH_4Cl system; (b) $(NH_4)_2SO_4$ system.

rapidly when the SF values in the NH_4Cl and the $(NH_4)_2SO_4$ systems were 0.93 and 0.96, respectively. The permeate flux decreased from 14.3 to 0 L/h/m² in 145 min in the NH_4Cl system. The corresponding SF_m was estimated at 1.07. Moreover, in the $(NH_4)_2SO_4$ system, the initial permeate flux is 12.6 L/h/m² followed by a sharp decrease to 0 L/h/m² within 130 min. The comparison of SEM micrographs between new and fouled membrane indicated that two kinds of ammonium salts resulted in two different kinds of membrane fouling, as shown in Figs. 9 and 10. In the NH_4Cl system, the deposition existed on both membrane surface and pore wall. As mentioned above, the volatile HCl could be generated in the acidic condition. The NH_4Cl particle was formed by the reaction between the volatile HCl and the volatile NH_3 and deposited on the membrane pore wall. This membrane fouling had direct effects on the membrane life due to its irreversibility. On the contrary, large amount of $(NH_4)_2SO_4$ crystal depositing on the membrane surface and little on the pore wall was observed. It could be interpreted by that the non-volatile SO_4^{2-} was rejected

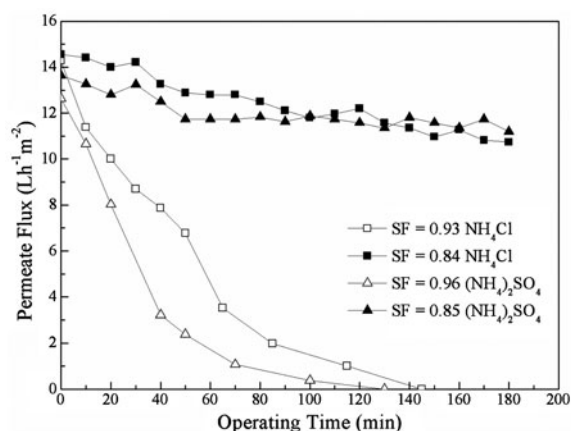


Fig. 8. The permeate flux vs. operating time as a fraction of feed SF (operating condition: $P_v=9$ kPa, $Q=90$ L/h, $T_f=333$ K).

by the hydrophobic membrane and no reaction occurred in membrane pore. Additionally, the concentration on the membrane surface has reached the supersaturation leading to $(NH_4)_2SO_4$ crystal accumulation. The permeate flux was recovered to the initial value as the distilled water was used to clean the membrane surface. Therefore, this kind of membrane fouling has less effect on the membrane life.

Consequently, the determining concentration in concentration, which was processed by VMD should be considered for preventing membrane fouling. According to Fig. 7, the R_f increased slowly when the SF_m was below the critical point. For that reason, the membrane fouling could be avoided before reaching the critical point. Therefore, the feed SF was investigated for the permeate flux behavior with the operating time in Fig. 8.

Fig. 8 illustrated that the permeate flux decreased slowly with the operating time as the SF values were 0.84 and 0.85 in the NH_4Cl and the $(NH_4)_2SO_4$ systems, respectively. The corresponding SF_m values in the NH_4Cl and the $(NH_4)_2SO_4$ systems were 0.95 and 0.93, respectively. The growth of membrane fouling could be limited as the feed concentration was below the critical point. However, in consideration of the balance between membrane fouling and the salt crystals recovery in the crystallizer, the determining concentration should not be too low. The SF (T_c) should be above 1 where T_c is the temperature in the crystallizer.

4.3. Crystallization process

Preliminary experiments on a batch crystallizer were performed using ammonium salt aqueous solutions concentrated by VMD process. The natural

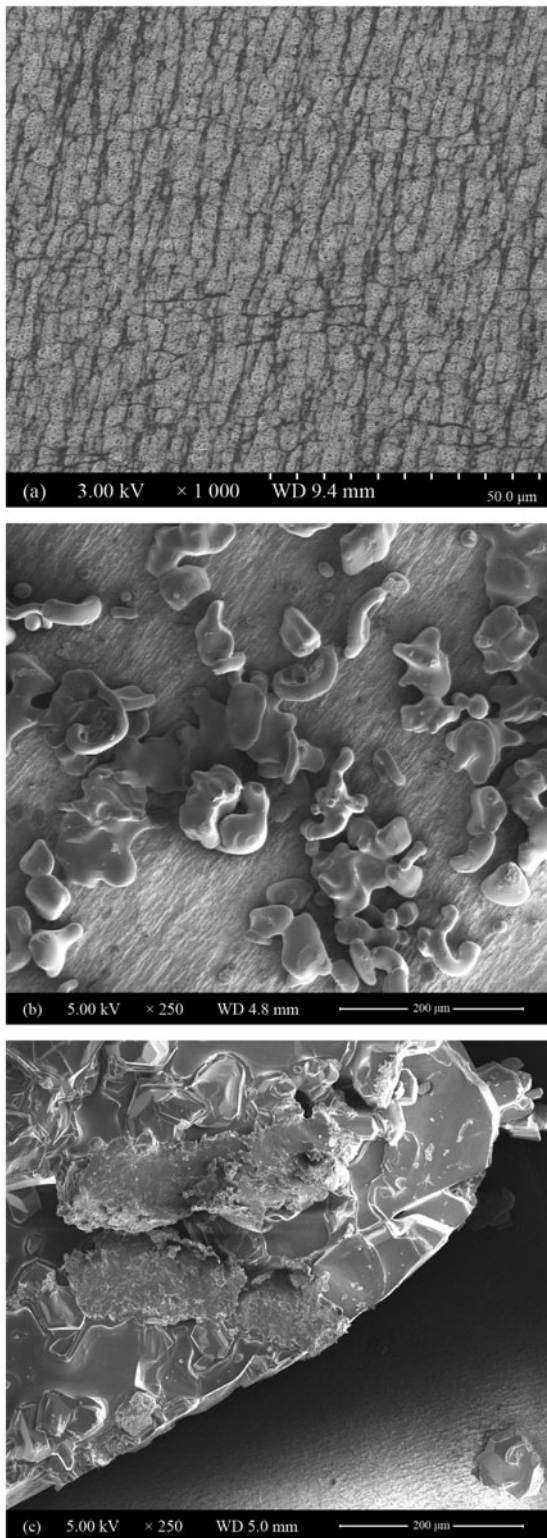


Fig. 9. SEM images of membrane surface: (a) new PTFE membrane; (b) fouled membrane with NH_4Cl system; (c) fouled membrane with $(\text{NH}_4)_2\text{SO}_4$ system.

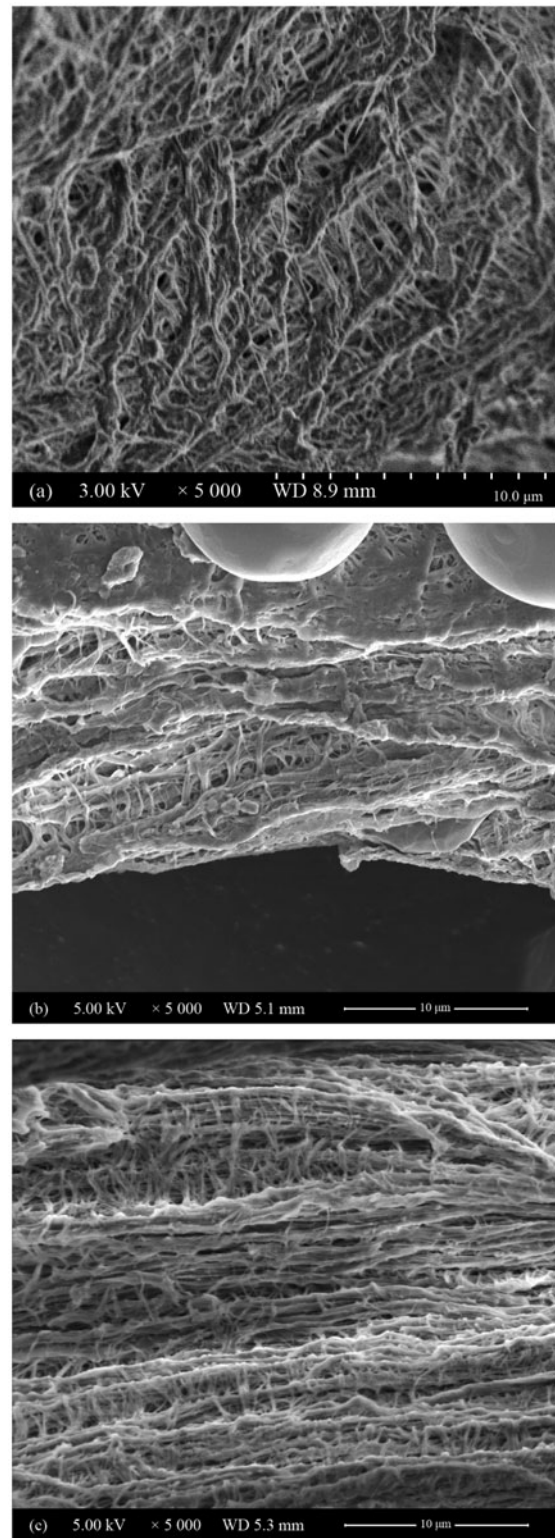


Fig. 10. SEM images of membrane pore wall: (a) new PTFE membrane; (b) fouled membrane with NH_4Cl system; (c) fouled membrane with $(\text{NH}_4)_2\text{SO}_4$ system.

Table 1
The crystal yields with different feed SF

NH ₄ Cl SF (333 K)	Crystal yield (kg/m ³)	(NH ₄) ₂ SO ₄ SF (333 K)	Crystal yield (kg/m ³)
0.78	78.9	0.85	37.8
0.82	108.6	0.89	47.7
0.87	125.7	0.91	58.4

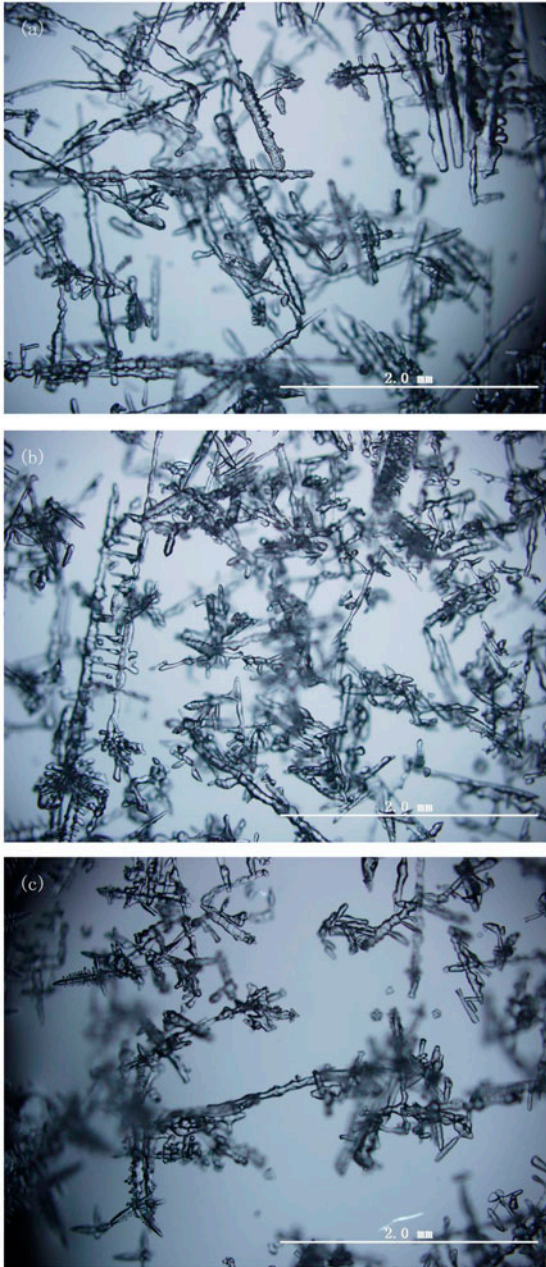


Fig. 11. Microscope images of the NH₄Cl crystal with different feed SF: (a) SF (333 K) = 0.78; (b) SF (333 K) = 0.82; (c) SF (333 K) = 0.87.

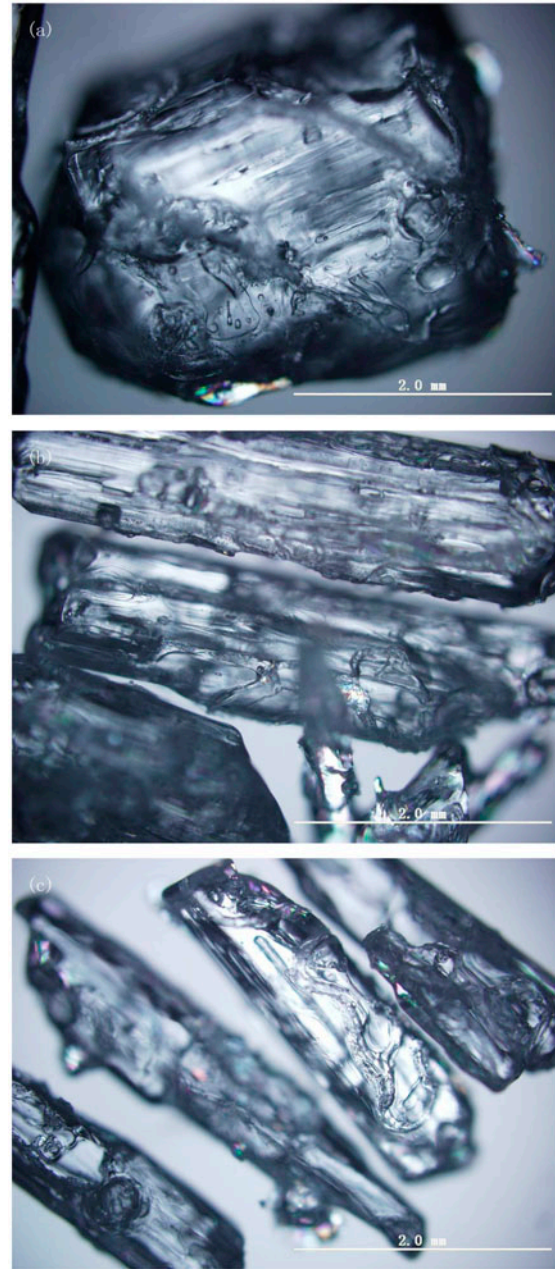


Fig. 12. Microscope images of the (NH₄)₂SO₄ crystal with different feed SF: (a) SF (333 K) = 0.85; (b) SF (333 K) = 0.89; (c) SF (333 K) = 0.91.

cooling mode was employed in this work. The final cooling temperature of the crystallized solution was 283 K. The yields of crystals under different SF (333 K) are presented in Table 1. It was observed that the yield would increase with the solution concentration.

The microscope images of the ammonium salt crystal with different solution concentrations are presented in Figs. 11 and 12. The dendritic structure of NH_4Cl crystals and the lamellar of $(\text{NH}_4)_2\text{SO}_4$ crystals were observed. The results indicated that the size of crystal decreased with the increasing solution concentration. Higher degree of supersaturation might result in larger amounts of crystal nucleus produced in short period. Therefore, the growth of the crystal nucleus was limited which lead to smaller size crystal.

4.4. Estimation of energy consumption

In the MDC process, heating of the feed solution was the main energy consumption. However, the permeate gas has large amount of thermal energy which could be recycled. As shown in Fig. 13, the supernatant of crystallizer was designed to flow back to the

MD process due to the decline of ammonia salt concentration. The permeate gas was transported to the heat exchanger for supernatant heating. Table 2 shows the estimation of the energy consumptions and recovery by Eqs. (15–17) in this MDC process (recycle MDC). Results showed that the theoretical recycle energy was significantly larger than the energy consumption. Therefore, high efficiency of energy recovery from permeate gas would reduce the required energy. Moreover, the backflow of the supernatant would increase the water recovery [7].

$$Q_t = C_w(T_{333} - T_{298}) \times m_f \quad (15)$$

$$\Delta_{\text{vap}}H_w(T_{323}, 9\text{kPa}) = \Delta H_w(T_{323}, 9\text{kPa}, \text{g}) - \Delta H_w(T_{323}, 9\text{kPa}, \text{l}) \quad (16)$$

$$Q_R = [C_w(T_{323} - T_{283}) + \Delta_{\text{vap}}H_w(T_{323}, 9\text{kPa})] \times m_p \quad (17)$$

where Q_t is the total energy used in feed solution heating (kJ), C_w is the heat capacity of water (4.2 kJ/kg/K), m_f is the mass of the feed solution (kg),

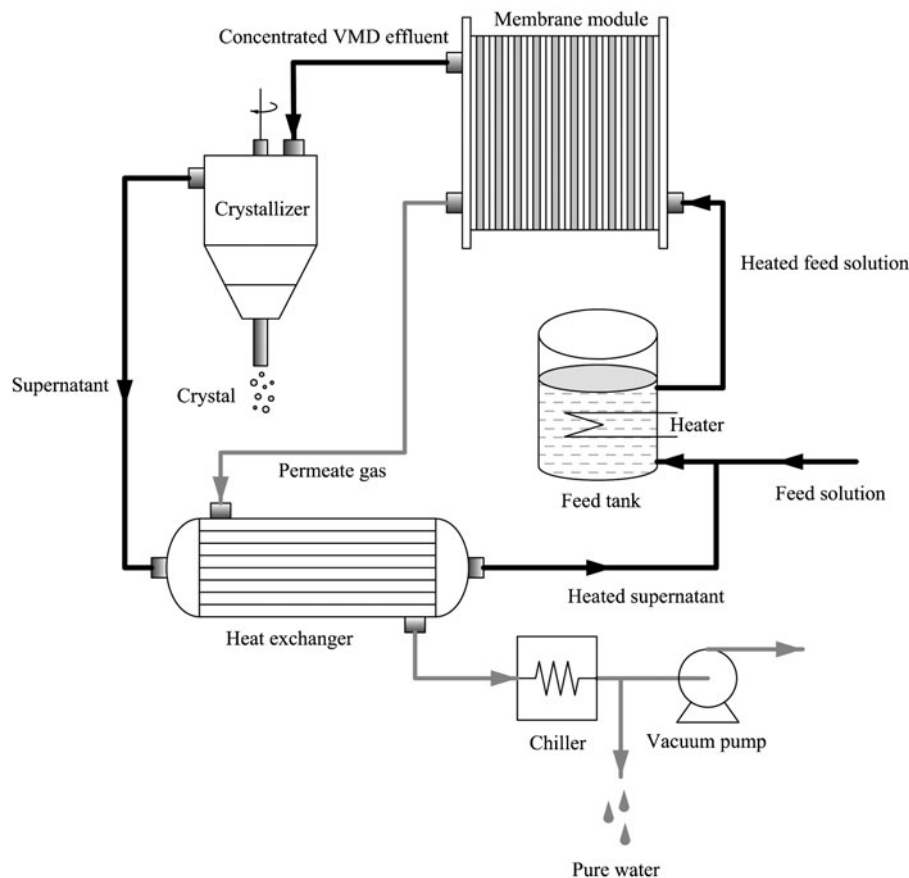


Fig. 13. Schematic diagram of the recycling MDC process.

Table 2
The estimation of energy consumption in the recycling MDC process

Parameters	Recycling MDC process
Initial temperature (K)	298
Operating temperature (K)	333
Concentration multiple	2
Estimated membrane temperature (K)	323
Temperature of cooled permeate liquid (K)	283
Theoretical heat energy consumption (kJ/m ³)	1.47 × 10 ⁵
Theoretical heat energy recovery (kJ/m ³)	1.25 × 10 ⁶

$\Delta H_w(T_{323}, 9 \text{ kPa}, 1)$ is the enthalpy of the liquid water (209.336 kJ/kg), $\Delta H_w(T_{323}, 9 \text{ kPa}, 1)$ is the enthalpy of gas water (2591.13 kJ/kg), Q_R is the recycle heat energy from permeate gas (kJ), and m_p is the mass of permeate (kg).

5. Conclusion

Ammonium salt solution was concentrated by VMD for recovering pure water and generating crystals in the crystallizer.

The initial permeate flux of 32 L/h/m² was obtained in the concentration process and decreased with the operating time. Batch crystallizer was carried out on the concentration solution, which lead to the production of 125.7 kg/m³ of NH₄Cl crystals and 58.4 kg/m³ of (NH₄)₂SO₄ crystals.

The permeate concentration of TN was affected by the negative ions of ammonia salt. In the NH₄Cl system, the permeated TN increased rapidly from 4.7 to 59.8 mg/L at the end of concentration experiment due to the volatile HCl and NH₃ passing through the membrane pore in acidic condition. However, the permeated TN with (NH₄)₂SO₄ solution was maintained at low level (TN < 3 mg/L) in the entire concentration process.

The transfer resistances were estimated by solving the developed model equations. Membrane fouling resistance slightly increased as the solution concentration reached up to a critical point. The membrane fouling was observed in both systems when the solution SF was beyond this critical point. The membrane fouling occurred by the deposition of (NH₄)₂SO₄ on the membrane surface was reversible. However, the irreversible membrane fouling was observed on both the membrane surface and the pore wall in the NH₄Cl system.

The recycle heat energy from the permeate gas was proven to be larger than the energy consumption of heating feed solution. Therefore, effective use of the permeate gas will reduce the total energy consumption.

Acknowledgments

The authors thank for financial support by the Key Technology R&D Program of Shanghai Committee of Science and Technology in China (11DZ1205201), Special Project of the Development and Industrialization of New Materials of National Development and Reform Commission in China (20132548), and the Key Technology R&D Program of Jiangsu Committee of Science and Technology in China (BE2013031).

Nomenclature

C	—	concentration (kg/m ³)
C	—	heat capacity (kJ/kg/K)
d_h	—	hydraulic diameter of channel (m)
D_{self}	—	diffusion coefficient (m ² /s)
h_f	—	heat transfer coefficient
ΔH	—	latent heat of vaporization (J/mol)
J	—	permeate flux (L/h/m ²)
k	—	mass transfer coefficient
K_m	—	membrane distillation coefficient
l	—	channel length (m)
M	—	molecular mass (mol/kg)
m	—	mass (kg)
Nu	—	Nusselt number
P	—	pressure (kPa)
P_{sat}	—	saturated vapor pressure (kPa)
Pr	—	Prandtl number
Q	—	quantity of heat (kJ/m ³)
r	—	size of membrane pore (m)
R	—	gas constant (J/mol/K)
	—	mass transfer resistance (Pa h ² /kg)
Re	—	Reynolds number
T	—	temperature (K)
v	—	solution velocity (m/s)
x	—	molar fraction

Greek letters

γ	—	activity coefficient
δ	—	membrane thickness (m)
ε	—	porosity of the membrane
μ	—	viscosity of feed solution (Pa s)
μ_w	—	viscosity of water (Pa s)
ρ	—	density of solution (kg/m ³)
τ	—	pore tortuosity

Subscripts

b	—	boundary layer
f	—	feed solution
m	—	membrane surface
p	—	permeate
R	—	recovery
t	—	total
v	—	permeate side
w	—	water

References

- [1] H.M. Huang, X.M. Xiao, B. Yan, Recycle use of magnesium ammonium phosphate to remove ammonium nitrogen from rare-earth wastewater, *Water Sci. Technol.* 59 (2009) 1093–1099.
- [2] S.W. Effler, C.M. Brooks, M.T. Auer, S.M. Doerr, Free ammonia and toxicity criteria in a polluted urban lake, *Res. J. Water Pollut. Control Fed.* 62 (1990) 771–779.
- [3] C.Y. Li, W.G. Li, G.Z. Wang, K. Wang, The preparation and the research of copper-chelex chitosan for removal ammonia-nitrogen from the drinking water, *Adv. Mater. Res.* 113–116 (2010) 1166–1169.
- [4] F. Edwie, T.S. Chung, Development of simultaneous membrane distillation–crystallization (SMDC) technology for treatment of saturated brine, *Chem. Eng. Sci.* 98 (2013) 160–172.
- [5] G.Q. Guan, R. Wang, F. Wicaksana, X. Yang, A.G. Fane, Analysis of membrane distillation crystallization system for high salinity brine treatment with zero discharge using aspen flowsheet simulation, *Ind. Eng. Chem. Res.* 51 (2012) 13405–13413.
- [6] R. Creusen, J. van Medevoort, Integrated membrane distillation–crystallization: Process design and cost estimations for seawater treatment and fluxes of single salt solutions, *Desalination* 323 (2013) 8–16.
- [7] M. Gryta, Concentration of NaCl solution by membrane distillation integrated with crystallization, *Sep. Sci. Technol.* 37 (2002) 3535–3558.
- [8] C.M. Tun, A.G. Fane, J.T. Matheickal, R. Sheikholeslami, Membrane distillation crystallization of concentrated salts—flux and crystal formation, *J. Membr. Sci.* 257 (2005) 144–155.
- [9] X. Ji, E. Curcio, S. Al Obaidani, G. Di Profio, E. Fontananova, E. Drioli, Membrane distillation–crystallization of seawater reverse osmosis brines, *Sep. Purif. Technol.* 71 (2010) 76–82.
- [10] S. Srisurichan, R. Jiraratananon, A.G. Fane, Mass transfer mechanisms and transport resistances in direct contact membrane distillation process, *J. Membr. Sci.* 277 (2006) 186–194.
- [11] A.M. Alklaibi, N. Lior, Heat and mass transfer resistance analysis of membrane distillation, *J. Membr. Sci.* 282 (2006) 362–369.
- [12] Z. Ding, L. Liu, J. Yu, R. Ma, Z. Yang, Concentrating the extract of traditional Chinese medicine by direct contact membrane distillation, *J. Membr. Sci.* 310 (2008) 539–549.
- [13] M.S. El-Bourawi, Z. Ding, R. Ma, M. Khayet, A framework for better understanding membrane distillation separation process, *J. Membr. Sci.* 285 (2006) 4–29.
- [14] K.W. Lawson, D.R. Lloyd, Membrane distillation, *J. Membr. Sci.* 124 (1997) 1–25.
- [15] R.W.A. Schofield, A.G. Fane, C.J.D. Fell, Heat and mass transfer in membrane distillation, *J. Membr. Sci.* 33 (1987) 299–313.
- [16] M. Khayet, M.P. Godino, J.I. Mengual, Theoretical and experimental studies on desalination using the sweeping gas membrane distillation method, *Desalination* 157 (2003) 297–305.
- [17] J.I. Mengual, M. Khayet, M.P. Godino, Heat and mass transfer in vacuum membrane distillation, *Int. J. Heat Mass Trans.* 47 (2004) 865–875.
- [18] A. Pano, E.J. Middlebrooks, Ammonia nitrogen removal in facultative wastewater stabilization ponds, *J. Water Pollut. Control Fed.* 54 (1982) 344–351.
- [19] P.H. Liao, A. Chen, K.V. Lo, Removal of nitrogen from swine manure wastewaters by ammonia stripping, *Bioresour. Technol.* 54 (1995) 17–20.
- [20] M.S. El-Bourawi, M. Khayet, R. Ma, Z. Ding, Z. Li, X. Zhang, Application of vacuum membrane distillation for ammonia removal, *J. Membr. Sci.* 301 (2007) 200–209.
- [21] D. Salavera, S.K. Chaudhari, X. Esteve, A. Coronas, Vapor–liquid equilibria of ammonia + water + potassium hydroxide and ammonia + water + sodium hydroxide solutions at temperatures from (293.15 to 353.15) K, *J. Chem. Eng. Data* 50 (2005) 471–476.
- [22] Z. Ding, L. Liu, Z. Li, R. Ma, Z. Yang, Experimental study of ammonia removal from water by membrane distillation (MD): The comparison of three configurations, *J. Membr. Sci.* 286 (2006) 93–103.
- [23] L. Martínez-Díez, F.J. Florido-Díaz, Desalination of brines by membrane distillation, *Desalination* 137 (2001) 267–273.